2950 Niles Road, St. Joseph, MI 49085-9659, USA
269.429.0300 fax 269.429.3852 hq@asabe.org www.asabe.org

An ASABE Meeting Presentation

Paper Number: 085111

Mode of Failure Model for Cutting Solid Section Biomass

David Lanning

Christopher Lanning

James Fridley, PhD, PE

James Dooley, PhD, PE

Mark DeTray

Forest Concepts, 3320 West Valley Hwy. N. D110, Auburn, WA 98001

Written for presentation at the
2008 ASABE Annual International Meeting
Sponsored by ASABE
Rhode Island Convention Center
Providence, Rhode Island
June 29 – July 2, 2008

Abstract. *Solid section biomass, such as wood and the node-zone of crop residues, has distinct modes of failure when loaded in cross grain shear. Shear bar design plays a part in determining what the failure mode will be at a given depth of penetration. Other factors include shear location relative to an unconstrained end and species type. In order to design a low energy consuming shear bar for agricultural and industrial machinery such as balers and choppers, one needs to develop a predictive model of the failure modes to minimize energy consumption. Utilizing a purpose built instrumented shear test apparatus, we have developed a set of equations and a governing model to predict failure mode and force required shearing solid section biomass. Our tests involved multiple cross sectional areas, 3 shear bar designs, and multiple cross sectional shapes.*

Keywords. Biomass, shear, failure mode, bale, solid section

Introduction

Size reduction is an energy consuming yet critical step in collection, handling and many uses of solid section biomass. Currently however, there is increasing concern regarding energy consumption and the need for energy efficient systems. One key to creating an energy efficient size reduction process is to understand the interactions of materials and the cutting mechanisms that act on them. We examined the anvil / shear bar mechanism for cross grain cutting of wood.

In order to conduct controlled experiments we developed The Dendromass Shearing Simulator (DSS). The DSS is a purpose built, fully instrumented shear testing apparatus, which can isolate and record the forces required to cut across the grain of fibrous cellulosic materials subjected to anvil / shear bar cutting.

We conducted a series of controlled experiments in the Forest Concepts LLC Auburn, Washington laboratory with the DSS. Our initial experiments failed to validate and extend existing models that predict shear forces for woody materials, yielding results that were inconsistent with those expected of pure cross grain shearing. A second group of data was collected in an effort to better understand the mechanism by which wood failed and to provide a basis for developing a new model. A third group of data was collected to validate the new model. In the last group of experiments, various configurations of blades were used.

Safety Emphasis

Shear bars in equipment tend to place large eccentric loads on machinery such as choppers and balers. Jams must be cleared and frequently trigger unsafe acts. Some modes of failure may result in chunks of biomass being thrown from the machine. As such, understanding and predicting forces and modes of failure will allow safer and more efficient machines to be designed.

In the DSS we use a screen between the operator and the material to protect from debris as well as preventing the operator from placing appendages in harms way. Samples are held in place by bungee cords rather than by the operator.

Background

Traditional beliefs dictate that when material is cut with a shear bar and anvil it fails in pure shear (defined later). Theory of pure shear states that blade geometries do not matter; the shear area alone affects the required force to complete the shearing operation. In our experiment we determined that pure shear alone is not adequate to describe solid section biomass cutting.

Description of Experiment

Equipment

The core of the experiment was the DSS machine (Figure 1). Developed and built exclusively for this test, it includes a LabView™ based software package to record data, a hydraulic power pack to provide smooth application of force, and three blades of different angles equal to 90, 45, and 22.5 degree (Figure 7). The three blades were attached to the sled with a single line of five 3/8” counter sunk cap screws to allow easy changing or replacement (Figure 2). The same bolt pattern is used to hold the stationary side of the shear. Each blade has 29.2 cm (11.5 in) long cutting edge, 1.2 cm (1/2 in) thick, and protrudes 5 cm (2 in) beyond the sled. The upper surface

of the blade (shearing surface) is 13 cm (5 1/8 in) above the removable sample support surface. The sled moves along two tracks, one on each side, and holds the blade to 0.08 +/- 0.08 cm (1/32 +/- 1/32 in) below the stationary shear bar. The tracks have load cells which detect the amount of force perpendicular to sled motion applied to the sled. Force is applied to the sled and subsequently to the blade by an 8.9 cm (3.5 in) diameter by 45.7 cm (18 in) stroke hydraulic cylinder. The attachment point on the cylinder is coplanar with the top of the blade on the sled and applies force parallel to the motion to minimize eccentric loading. The hydraulic system moves the sled moves at 1.52 cm/s (0.60 in/s) and delivers up to 85.6 kN (19250 lbs) of force to the blade.

Force applied to the sled is measured through a pressure transducer on the hydraulic circuit. Position is measured by an analog pullout cable sensor providing near infinite resolution. Position zero is the point at which the blade and the bypass anvil cross. A negative number indicates the distance remaining to intersection, and a positive number indicates the amount of overlap. The vertical reaction forces are measured by the load cells along the side tracks as previously described. Knowing the position of the load cells, the position of the sled and recording input from each cell independently allows us to calculate the bending force on the blade and to correct for blade, sled, and cylinder / oil weight through the range of sled motion.

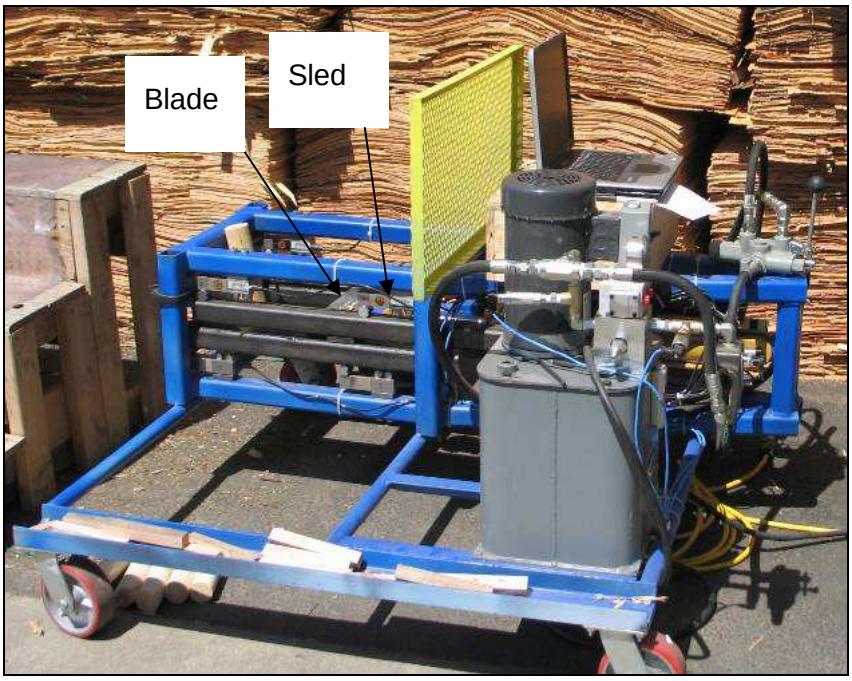

Figure 1: DSS testing apparatus.

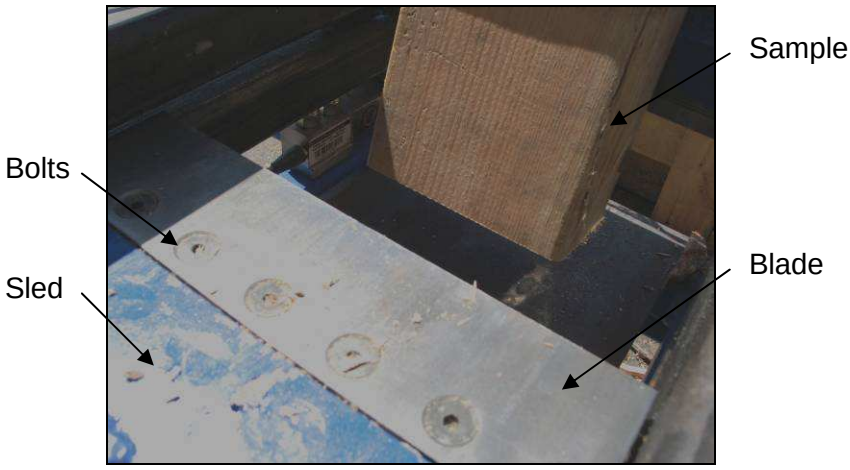

Figure 2: Shear blade attachment

Samples

Samples were prepared in two different ways. Some samples were cut an arbitrary length with cross sections including a range of round wood diameters and some typical construction grade lumber. Other samples of 2.5 cm x 2.5 cm by 30.5 cm long (1 x 1 x 12 in) were cut from low grade 2x4's. A complete list of samples is shown in Table 1 and Table 2. Moisture content was not measured but was assumed to be about 9% wwb (equilibrium moisture content in Seattle, Washington) as samples were stored in a closed unheated environment before use.

Table 1: Size and quantity of rectangular type samples, typically Douglas fir samples.

Depth (cm)	Width (cm)	Length (cm)	Qty
2.5	2.5	30.5	90
3.8	8.9	30.5	14
8.9	8.9	30.5	3
8.9	14.0	30.5	1

Table 2: Size and quantity of round wood samples, all cut from lodge pole pine.

Nominal D (cm)	Actual D (cm)	Length (cm)	Qty
5.08	4.8	40.6	15
5.08	4.8	61.0	3
6.35	6.4	45.7	9
7.62	8.4	30.5	9
7.62	8.4	61.0	3
10.16	9.9	61.0	6
12.7	12.2	61.0	3

Protocol

The experiment consisted of a group of two experimental setups with three runs conducted in each setup. Each run included one 2x4 sample. In the first setup, samples were sheared with the grain perpendicular the top plane of the blade with the sample resting on the bottom plate

(Figure 3). In the second, samples were suspended slightly above the bottom plate in the same orientation as the first samples. Data from this experiment was used to asses the pure shear model and to explore the influence of the bottom plate on the shear forces and failure mechanisms. We discovered that the pure shear model did not fit the data.

A second group of tests was used to determine if failure mode further explained the relationship between shear force and material as the cut occurred. These tests included stacks of 2.5 cm x 2.5 cm sections increasing in the number of sections in width with each run (a stack is similar to a laminate beam with out adhesive). The test was repeated with and increased number of sections in depth. A set of tests were also run with round wood samples. A new model was then developed.

A third and final group of round wood samples were tested specifically to verify the new model. Protocol was consistent with previous runs.

Data analysis method

The data recorded from each set was subsequently filtered by our specially developed data reduction and re-sampling software. The application averaged sequential groups of four data points, reducing the sample rate from approximately 12 Hz to 3 Hz while maintaining continuous integration, and produced a new data set with the reduced points. The frequency reduction helped reduce high frequency signal noise generated by the load cells and other sensors. After the data was re-sampled, data pertinent to this experiment (data where the knife is moving) was again filtered, removing the “dead time” from the data set. Each run’s highest recorded force in both axes and the position at which the highest force in the x-direction occurred were tabulated along with the area of the sample, orientation, blade configuration, and other parameters. Table 3 (in Appendix) contains information about the rectangular shaped samples and Table 4 (in Appendix) contains information about the round wood samples.

Results and Analysis

The initial model for cross grain shearing consists of a stationary anvil and a moving shear knife with the material to be sheared situated in between the two. It was suggested that the cross-sectional area of the wood to be cut would fail in fully constrained, perpendicular to grain shear, much like large shear press (Figure 4) or a screw cutter. The mathematical representation of the model is:

$$F = A_s \tau_{\perp}$$

Equation 1

Where:

F = The force required to shear

A_s = The shear area

$\tau_{\perp}$ = The shear strength perpendicular to grain of the material to be processed.

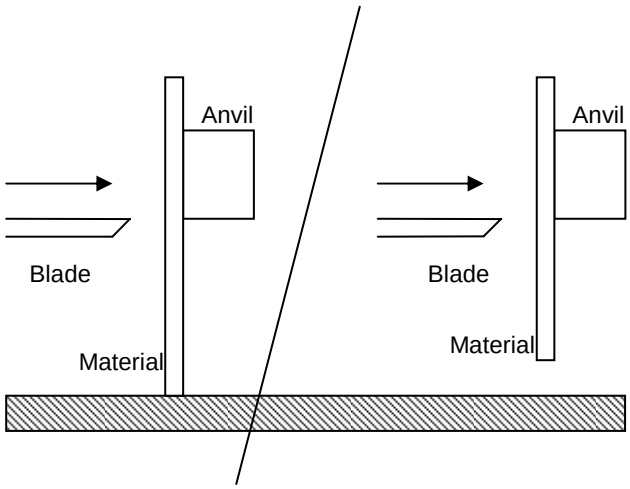

Figure 3 Left: Material sample resting on floor. Right: Material sample suspended above floor.

The first group of setups tested the significance of having the sample rest on the floor of the DSS (Figure 3). Figure 5 shows the results of the two runs. The first setup, with the samples resting on the floor averaged a maximum force of 31.4 kN (7058 pounds) while the second setup, with the samples suspended averaged 36.7 kN (8256 pounds). There is no significant difference in the force between the sets (p = 0.05).

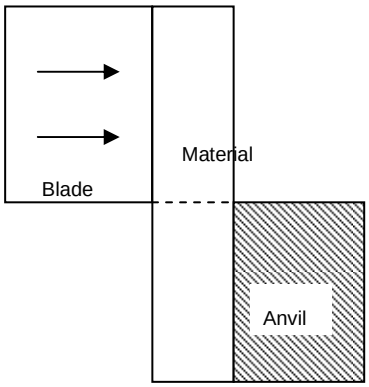

Figure 4 Initial model diagram. Blade moves left to right shearing material along dashed line.

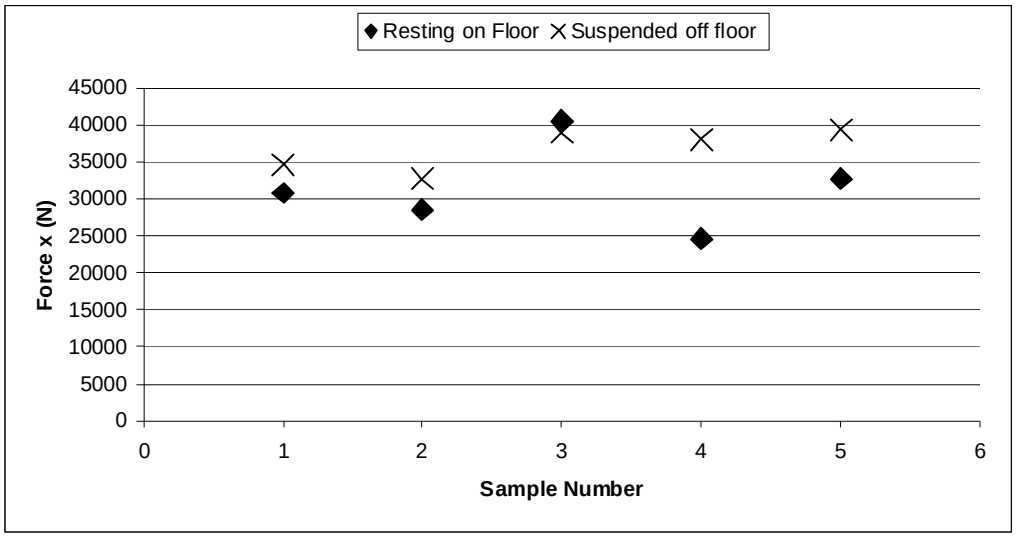

Figure 5: Comparison of similar cross section resting on floor or suspended above floor.

The next group of tests was to determine if there was a pattern in the way the cut occurred. They include the build up of 2.5 cm x 2.5 cm sections and round wood. Figure 6 shows the shear area vs. maximum force required; a loose trend can be seen. Best fit was a linear relationship with an R^2 of 0.80. Though the model would yield reasonably accurate predictions for failure forces, it was inconsistent with the visual inspection of failure modes (Figure 8).

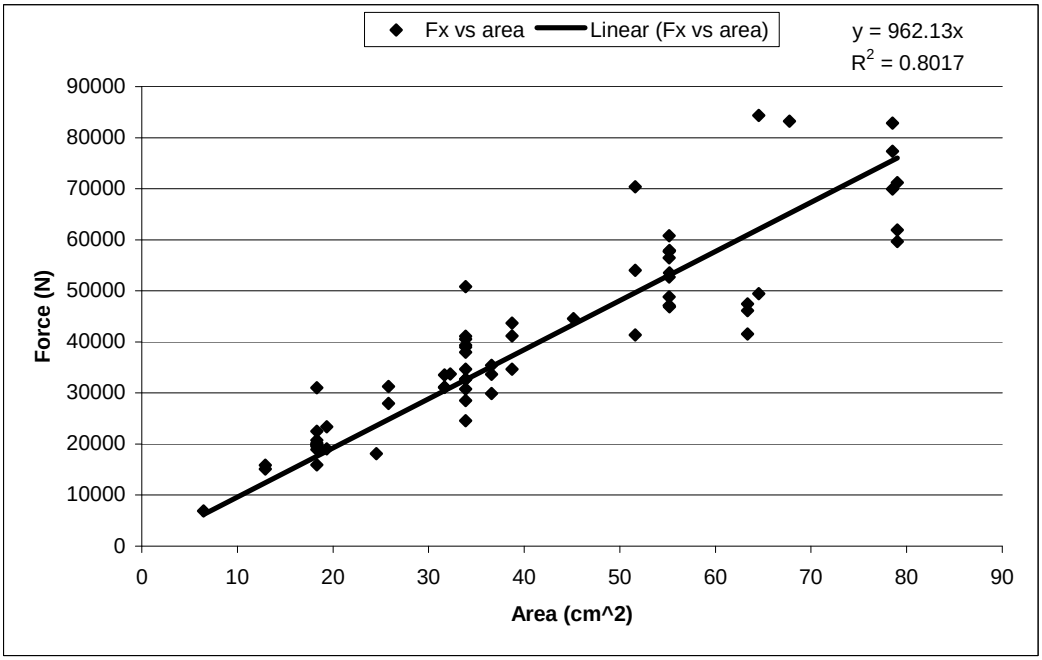

Figure 6: Shear area vs. maximum force.

A new model as follows was developed that appeared to fit with the collected data (visual inspection of failed material as well as tested force values); a third group of tests was developed to validate the new model. The follow equations refer to the dimensions shown in Figure 7.

Material Properties used:

$\sigma_{//T}$ = Maximum stress parallel to grain in tension.

$\sigma_{//C}$ = Maximum stress parallel to grain in compression.

$\sigma_{\perp C}$ = Maximum stress perpendicular to grain in compression.

$\tau_{//}$ = Maximum shear stress parallel to grain

E = Modulus of elasticity

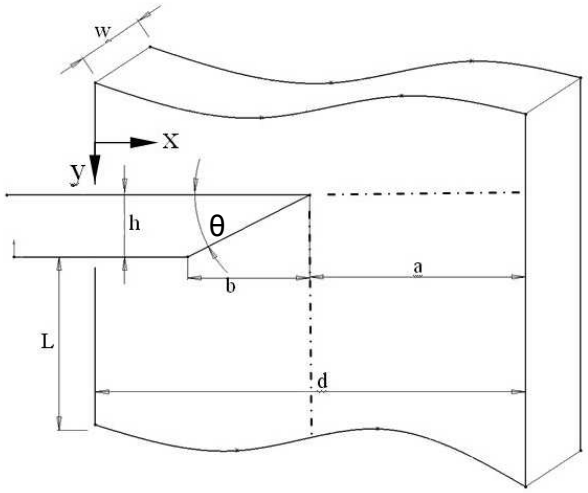

Figure 7: Variables used in the size reduction system model.

Our experiment showed us that fibrous materials such as wood, when cut with a knife or similar, do not fail in shear so much as in tension. The knife acts as a wedge which slowly drives the material apart. While rarely understood, this is the principle of wood chippers. As the knife is pressed deeper into the material, not only does the force generated from the displacement of the material increase, but the area of the remaining material decreases, thus when the stress in the remaining material surpasses the maximum stress parallel to grain in tension, the piece fails. The force necessary to complete the process is related the force generated along the slope of the blade and friction developed along the blade.

Failure occurs when the stress in the remaining portion of material is greater than the maximum stress parallel to grain in tension. The maximum force the remaining portion can resist then is:

$$F_{a\max} = \sigma_{//T} A_a = \sigma_{//T} aw$$

Equation 2

Where:

$F_{a\max}$ = The maximum force remaining portion can resist

A_a = The remaining uncut area

a = The uncut depth

w = The material piece width

And

$$A_a = d - x$$

Equation 3

Where:

d = The total piece depth

x = The depth of blade penetration

Therefore

$$F_{a\max} = \sigma_{//T}(d - x)w$$

Equation 4

Force induced in the remainder is the sum of the force developed on the slope and flat parts of the blade.

$$F_y = F_{yslope} + F_{flat}$$

Equation 5

Where:

F_y = The force induced in the remaining portion

F_{yslope} = The forced developed by the sloped portion of the blade in the y direction

F_{flat} = The force developed by the flat part of the blade in the y direction

The force against the blade arises from the deflection (compression) of the material which is directly proportional to the strain rate and length of the specimen

$$\delta = \varepsilon L$$

Equation 6

Where:

δ = The deflection

ε = The strain

L = The length of material

In this case, the deflection is known, length and strain rate are not. However, Hooke's law says:

$$\varepsilon = \frac{\sigma}{E}$$

Equation 7

Where:

σ = The stress in the uncut portion of material

With

$$\sigma = \frac{F_y}{A_a}$$

Equation 8

And

$$\varepsilon = \frac{F_y}{EA_a}$$

Equation 9

Then δ becomes

$$\delta = \frac{F_y L}{EA_a}$$

Equation 10

Where:

L shall be further defined as the material length from the cutting edge to an end in the direction of the bevel side of the blade

Now *L* is somewhat of a challenge in that only part of the piece length actually is affected by the presence of the knife. There is a minimum length, however, as determined by the relationship between the shear strength parallel to grain and the tensile strength parallel to grain. For failure to occur in the tension parallel to grain in the remaining portion there must be sufficient area along L for the shear to act on such that the shear force equals the force needed for tensile failure. That minimum area determines the characteristic length *L*. Interestingly, though not included in this study, it can be argued that if material is sufficiently constrained by resting on the floor plate that material will fail as if an infinitely long length, provided that the piece is sufficiently long to absorb the compression caused by blade thickness.

$$\tau_{//} A_s = \sigma_{//T} A_a$$

Equation 11

Where:

A_s = The shear area acted upon parallel to grain

Rewritten and expanded

$$\tau_{ll} Lw = \sigma_{//T} aw$$

Equation 12

Solving for *L*, the minimum length, and substitute using Equation 3 yields

$$L = \frac{\sigma_{//T}(d - x)}{\tau_{//}}$$

Equation 13

When *L* is substituted back into Equation 10

$$\delta = \frac{F_y \sigma_{//T} (d - x)}{E A_a \tau_{//}}$$

Equation 14

Solving for the force, we see that for every x position there is one force.

$$F_y = \frac{\delta E A_a \tau_{//}}{\sigma_{//T} (d - x)}$$

Equation 15

However, because the blade has more than one plane, a piece-wise function is needed to describe the deflection. One function for the blade as it is enters along the angle, and a second for the extension of the blade as the maximum thickness is reached. For $0 \le x \le b$ where the displacement varies along the length of penetration

$$\delta = x \tan(\theta)$$

Equation 16

Where:

θ = The blade angle as measured horizontal to the blade bevel

The average displacement is $\frac{\delta}{2}$ and because hooks law is a linear relationship, an average value is valid. Also, the area involved in this portion is simple xw because it is the projected area under consideration. Therefore, for $0 \le x \le b$

$$F_{yslope} = \frac{x \tan(\theta) E x w \tau_{//}}{2\sigma_{//T} (d - x)} \Rightarrow \frac{x^2 \tan(\theta) E w \tau_{//}}{2\sigma_{//T} (d - x)}$$

Equation 17

For the sloped portion of the force, once the penetration distance *x* has tapered length *b*, then the force due to the sloped portion no longer increases with the slope, but does increase with the diminishing characteristic length *L*. For $x \ge b$

$$F_{yslope} = \frac{h b E w \tau_{//}}{2\sigma_{//T} (d - x)}$$

Equation 18

Where:

h = The blade thickness

b = The depth of blade bevel in the x direction

Until $x \geq b$ the Force due to the flat portion of the knife is zero, but afterward the displacement is constant in the form

$$F_{flat} = \frac{h(x-b)Ew\tau_{//}}{\sigma_{//T}(d-x)}$$

Equation 19

From Equation 5, the total down force for $0 \leq x \leq b$

$$F_y = 0 + \frac{x^2 \tan(\theta)Ew\tau_{//}}{2\sigma_{//T}(d-x)}$$

Equation 20

Similarly for $x \geq b$ the total force is

$$F_y = \frac{h(x-b)Ew\tau_{//}}{\sigma_{//T}(d-x)} + \frac{hbEw\tau_{//}}{2\sigma_{//T}(d-x)}$$

Equation 21

There is limit to the amount of resistant force that can be applied by the knife, which is the maximum stress parallel to grain limit. Without sufficient area to carry the load, a high force will locally buckle to relieve the stress. The force exerted by a section of blade is limited by the area of that section and the properties of the material. For instance, for $0 \leq x \leq b$ where only the sloped part is involved and using Equation 8

$$F_{yslope,\max} = \sigma_{\perp C} xw$$

Equation 22

Where:

$F_{yslope,\max}$ = The maximum force in the y direction achievable by the sloped portion of the blade

For $x \geq b$ the force down on the flat is limited to

$$F_{flat,\max} = \sigma_{\perp C}(x-b)w$$

Equation 23

Where:

$F_{flat,\max}$ = The maximum force in the y direction achievable by the flat portion of the blade

And for $x \geq b$ the total force down on the blade is limited to

$$F_{y,\max} = \sigma_{\perp C}(x-b)w + \sigma_{\perp C} bw = \sigma_{\perp C} w(x-b+b) = \sigma_{\perp C} wx$$

Equation 24

Where:

$F_{y,\max}$ = The maximum achievable force in the y direction on the blade

While in many cases, the failure point can be determined exclusively by Equation 24, the forces calculated by component are important in relation to the force applied in the *x* direction or, the force necessary to push the knife into the material. The most obvious force is the component of the F_{slope} that is in the *x* direction

$$F_{xslope} = F_{yslope} \frac{b}{h}$$

Equation 25

Where:

F_{xslope} = The force in the x direction developed by the sloped portion of the blade

Where F_{yslope} is the lesser of the calculated F_{yslope} or $F_{yslope,\max}$. However, like the forces in the *y* direction, there is a limit to the component in the *x* direction governed by the material's maximum compressible stress perpendicular to the grain and the area over which the force acts.

$$F_{xslope,\max} = \sigma_{\perp C} hw$$

Equation 26

Where:

$F_{xslope,\max}$ = The maximum achievable force in the x direction on the slope of the blade

A less obvious, yet still significant, component is the friction developed along the depth of the blade. The friction along each component can be added where the force of friction is equal to the normal force F_N on that surface times the coefficient of friction *Cf*, note that the normal force is no more that the maximum force on that surface as determined by Equation 22, Equation 23, Equation 24 or Equation 26.

$$F_f = F_N Cf$$

Equation 27

Where:

F_f = The force of friction resistance in the x direction

F_N = The normal force on the blade surface

Cf = The coefficient of friction between the material and the blade

The total friction resistance in the *x*-direction is the summation of each of the components' *x*-direction contribution.

$$F_f = F_{f,xslope} + F_{f,flat} + F_{f,top}$$

Equation 28

Where:

$F_{f,xslope}$ = The force of friction resistance in the x direction on the sloped portion of the blade

$F_{f,flat}$ = The force of friction resistance in the x direction on the flat (lower) portion of the blade

$F_{f,top}$ = The force of friction resistance in the x direction on the top of the blade

Individually, the total friction on the slope is

$$F_{f,slope} = F_N Cf = \sqrt{F_{yslope}{}^2 + F_{xslope}{}^2}\, Cf$$

Equation 29

But the component of the friction on the slope in the *x* direction is

$$F_{f,xslope} = F_N Cf \cos(\theta) = \sqrt{F_{yslope}{}^2 + F_{xslope}{}^2}\, Cf \cos(\theta)$$

Equation 30

And on the flat, the total friction is along the *x*-direction

$$F_{f,flat} = F_N Cf = F_{flat} Cf$$

Equation 31

Similarly, the full friction of the top is in the *x*-direction

$$F_{f,top} = F_N Cf = F_y Cf$$

Equation 32

Thusly, the total force applied (x direction) required to cut a solid section material is given by

$$F_{x-total} = \sqrt{(\sigma_{\perp C} xw)^2 + (\sigma_{\perp C} hw)^2}\, Cf \cos(\theta) + \sigma_{\perp C}(x-b)wCf + \sigma_{\perp C} wxCf$$

Equation 33

Where:

$F_{x-total}$ = The total force required in the x direction to cut a piece of material

All of the equations thus far apply to cutting a rectangular block of material and produce reasonably accurate results for the force needed to cut the material; however position indicated at failure may not be entirely accurate based on current tests. The equations apply to non rectangular sections as well. However the width *w* needs to be expressed as a function of *x*.

Discussion

The initial group of tests revealed that while the position of the failure changed, the amount of force did not as a result of the sample resting on the floor plate or suspended (see Figure 5). Because of this, subsequent cuts were made on or off the floor depending on which was easier to apply. While that detail was recorded with the data, it was ignored in the evaluation of the results as related to the force required in the x-direction. Also, as noted earlier, the force needed to cut the 2x4s was significantly less than predicted by our original model.

One particular observation, consistent with groups one and two, led to the development of the new model. That is, upon inspecting the two sides of the cut material, it appeared that while part of the material was marred by the knife, a portion of if failed in tension (Figure 8), not in shear as stated in the starting model. The first portion of the cut is simply the blade smashing into the side of the wood (see Figure 9 and Figure 10). If the piece is short, the perpendicular to grain tensile stress and the parallel to grain shear stress limits can be surpassed allowing pieces of the wood to flake off (Figure 10) as the knife proceeds. By taking into account various properties of wood that are readily available from the Wood Handbook and friction, a reasonably accurate model was developed. A third group of data sets were collected to verify the model. Figure 11 shows that the model and the data closely match. The model curve was also correlated back to all of the previously collected data by adapting the line of best fit from Figure 6 into an equivalent radius curve as shown in Figure 11. The model appears to fit over a wide variety of samples.

Figure 8: Catastrophic failure from parallel to grain tension, not shear.

Figure 9: The blade starts to cut by causing local compression failure.

Figure 10 Here it can be seen that there is significant compression failure in the region near the blade and whereever there is a force applied to resist the block movement.

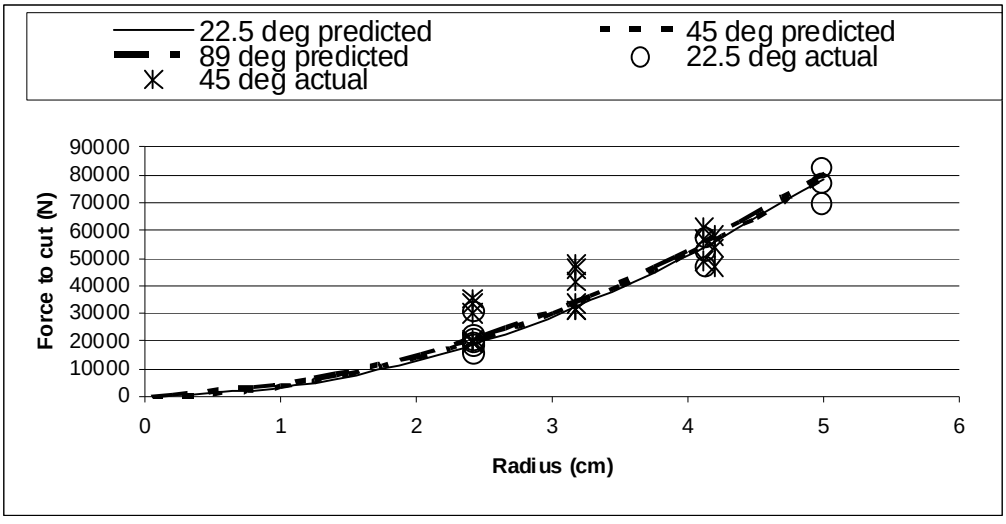

Figure 11 Third set results compared to model values for 2 blade angles. The third blade angle is shown as hypothesized, but not tested.

A very counterintuitive discovery was made in the testing of the model. While it would seem that a sharp blade would cut through the wood more readily, it actually makes very little difference. The majority of the resistant force is actually friction which the blade angle has little effect on. According to the model, in a configuration with a 12.5mm (0.50 in) thick blade and an 89 degree blade angle (nearly a square end) the total force on the blade at failure would be about 80 kN while only 7 kN arose from the force of resistance to the face of the blade. With all else the same, a blade angle of just 22.5 degrees gives a total resistance of 78 kN and only 6 kN is from the blade slope. With this type of cellulosic fibrous material the stress perpendicular to the grain is quickly overcome and the wood fails locally in compression.

A significant reduction in force required was achieved by replacing the square block stationary side (50mm (2 in) vertical face) of the machine with another blade (a blade having a 12.5mm (0.50 in) vertical face). In the two blade system, the force required to cut the material was reduced by more than 20% on average with round section of 50mm (2 in) radius. The percent reduction actually increases with an increase in diameter (see Figure 12).

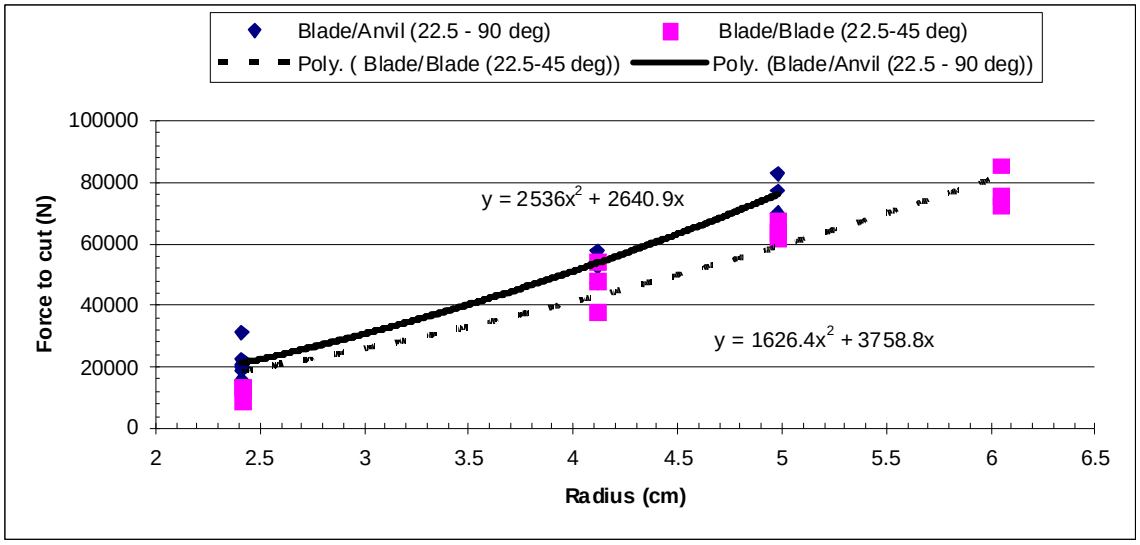

Figure 12 One blade and two blade configurations vs. maximum force to cut the material.

An easily overlooked yet important design aspect is that the blade must have sufficient depth to span the material. If the blade bottoms out per say (material hits blade support, effectively increasing the blade thickness) before the cut is complete, there is an immediate jump in the force required to complete the cut. When the blade bottoms out, the failure mode changes from local crushing, which results in a wedging effect, to a true shear where the remaining portion of wood must all be sheared simultaneously.

Conclusion

Solid section biomass, such as wood and the node-zone of crop residues, has distinct modes of failure when loaded in cross grain shear. While basic shear bar design plays a part in determining what the failure mode will be at a given depth of penetration, the sharpness of that blade is insignificant when compared to the affects of blade thickness and depth of penetration. Additionally the design of the surface opposing the blade is significant; a second blade instead of a bypass anvil is more efficient.

Other factors include shear bar location relative to an unconstrained end and species type. In order to design a low energy consuming shear bar for agricultural and industrial machinery such

as balers and choppers, one may use the model developed to predict the failure mode of the material and design a process based on the a desired piece size and anticipated failure mode. The model characteristic length L given in Equation 13 is the minimum length to cause failure in tension parallel to grain instead of flaking off portions of material.

$$L = \frac{\sigma_{//T}(d-x)}{\tau_{//}}$$

Equation 13 (repeat)

Equation 33 gives the maximum required force in the x direction to cause failure in the material.

$$F_{x-total} = \sqrt{(\sigma_{\perp C} xw)^2 + (\sigma_{\perp C} hw)^2}\, Cf\, \cos(\theta) + \sigma_{\perp C}(x-b)wCf + \sigma_{\perp C} wxCf$$

Equation 33 (repeat)

The most energy efficient solid section biomass cutting system would consist of two very thin blades with sufficient material penetration depth.

Future studies should examine blade various blade thicknesses ranging from very thin to very thick where relative thickness is determined by the material being cut. In the case of wood blades may range from 0.3cm (1/8 in) to 2.54cm (1 in). Additional studies may include determining the required material properties of other solid section materials such as corn stover nodes.

Acknowledgements

Development was supported in-part by the CSREES Small Business Innovation Research program of the U.S. Department of Agriculture, grant number # 2005-33610-15483 and # 2006-33610-17595.

References

1. Kachigan, S.K., *Multivariate Statistical Analysis - A Conceptual Introduction*. Second ed. 1991, New York: Radius Press. 303.
2. Forest Products Laboratory, *Wood Handbook - Wood as an Engineering Material*. 2002, Almonte, Ontario Canada: Algrove Publishing Limited. 464.
3. Persson, S. 1987. *Mechanics of Cutting Plant Material*. St. Joseph, MI: American Society of Agricultural Engineers.
4. Womac, A.R., M. Yu, C. Igathinathane, P. Ye, D. Hayes, S. Narayan, S. Sokhansanj, and L. Wright. 2005. Shearing characteristics of biomass for size reduction. ASAE Paper 056058. St. Joseph, MI: ASABE.

Appendix

Table 3: Tabulation of rectangular cross section wood sample results.

Position at Fx max.	F_x max	F_y max	blade config	Area	Configuration Width	Depth	R	description	floor

-0.70	6920	-2061	45-90	5.25	3.5	1.5	-	2x4	y
-0.66	6405	-1118	45-90	5.25	3.5	1.5	-	2x4	y
-0.62	9108	-2210	45-90	5.25	3.5	1.5	-	2x4	y
-0.57	5518	-1323	45-90	5.25	3.5	1.5	-	2x4	y
-0.52	7338	-2187	45-90	5.25	3.5	1.5	-	2x4	y
-0.85	7785	-2956	45-90	5.25	3.5	1.5	-	2x4	n
-0.82	7356	-2132	45-90	5.25	3.5	1.5	-	2x4	n
-0.79	8760	-2478	45-90	5.25	3.5	1.5	-	2x4	n
-0.78	8541	-2973	45-90	5.25	3.5	1.5	-	2x4	n
-0.78	8840	-2587	45-90	5.25	3.5	1.5	-	2x4	n
-0.64	11117	-1221	45-90	10	2	5	-	1x1 (10)	y
-1.00	9290	-1376	45-90	8	2	4	-	1x1 (8)	y
-1.03	9253	-1700	45-90	6	2	3	-	1x1 (6)	y
-0.73	7022	-1249	45-90	4	2	2	-	1x1 (4)	y
-0.49	3392	-647	45-90	2	2	1	-	1x1 (2)	y
-0.79	15822	-2522	45-90	8	4	2	-	1x1 (8)	y
-0.43	18964	-3602	45-90	10	5	2	-	1x1 (10)	y
-0.67	7581	-1404	45-90	5	5	1	-	1x1 (5)	y
-0.65	5259	-1200	45-90	3	3	1	-	1x1 (3)	y
-0.61	12147	-2296	45-90	8	8	1	-	1x1 (8)	y
-0.60	10018	-2514	45-90	7	7	1	-	1x1 (7)	y
-0.60	7795	-1500	45-90	6	6	1	-	1x1 (6)	y
-0.60	6280	-1046	45-90	4	4	1	-	1x1 (4)	y
-0.59	3563	-887	45-90	2	2	1	-	1x1 (2)	y
-0.55	1550	-452	45-90	1	1	1	-	1x1	y
-0.65	9820	-2240	45-90	6	3	2	-	1x1 (6)	y
-0.45	4280	-873	45-90	3	3	1	-	1x1 (3)	y
-0.76	11419	-1572	45-90	5.25	3.5	1.5	-	2x4	y
-0.85	18703	-3528	45-90	10.5	7	1.5	-	2x4 (2)	n
-0.84	9243	-2292	45-90	5.25	3.5	1.5	-	2x4	n
-2.03	13411	-4274	45-90	12.25	3.5	3.5	-	4x4	n
-1.31	16000	-3972	45-90	12.25	3.5	3.5	-	4x4	n
-2.28	13910	-3578	45-90	12.25	3.5	3.5	-	4x4	n
-1.81	19198	-5280	45-90	19.25	3.5	5.5	-	4x6	n

Table 4 Tabulation of round cross section wood sample results.

Position at Fx max	Fx max	Fy max	Configuration Blade	Area	Width	Depth	R	description	floor
-0.72	1929	-416	22.5-45	2.84	-	-	0.95	2" round	n
-1.16	2978	-368	22.5-45	2.84	-	-	0.95	2" round	n
-1.27	3074	-372	22.5-45	2.84	-	-	0.95	2" round	n
-1.58	8518	-1029	22.5-45	8.55	-	-	1.62	3" round	n
-1.28	10803	-2170	22.5-45	8.55	-	-	1.62	3" round	n
-1.22	12233	-1918	22.5-45	8.55	-	-	1.62	3" round	n
-1.63	13951	-1993	22.5-45	12.17	-	-	1.96	4" round	n
-0.65	14290	-2735	22.5-45	12.17	-	-	1.96	4" round	n

-1.15	15175	-2797	22.5-45	12.17	-	-	1.96	4" round	n
-2.34	16288	-1348	22.5-45	17.72	-	-	2.38	5"round	n
-2.23	16977	-970	22.5-45	17.72	-	-	2.38	5"round	n
-1.51	19198	-2561	22.5-45	17.72	-	-	2.38	5"round	n
-1.58	3575	-695	22.5-90	2.84	-	-	0.95	2" round	n
-1.51	4254	-1200	22.5-90	2.84	-	-	0.95	2" round	n
-0.90	4476	-1904	22.5-90	2.84	-	-	0.95	2" round	n
-0.87	4667	-1564	22.5-90	2.84	-	-	0.95	2" round	n
-0.80	5051	-1706	22.5-90	2.84	-	-	0.95	2" round	n
-1.08	6979	-1520	22.5-90	2.84	-	-	0.95	2" round	n
-2.06	10596	-1709	22.5-90	8.55	-	-	1.62	3" round	n
-2.01	11838	1188	22.5-90	8.55	-	-	1.62	3" round	n
-1.50	12967	-3033	22.5-90	8.55	-	-	1.62	3" round	n
-2.08	15714	-4219	22.5-90	12.17	-	-	1.96	4" round	n
-0.96	17377	2082	22.5-90	12.17	-	-	1.96	4" round	n
-0.86	18623	427	22.5-90	12.17	-	-	1.96	4" round	n
-0.89	4397	-1713	45-90	2.84	-	-	0.95	2" round	n
-0.87	4446	-1251	45-90	2.84	-	-	0.95	2" round	n
-0.84	4531	-1500	45-90	2.84	-	-	0.95	2" round	n
-0.97	4065	-1229	45-90	4.91	-	-	1.25	2.5" round	n
-1.22	6988	-1443	45-90	4.91	-	-	1.25	2.5" round	n
-1.40	6995	-2445	45-90	4.91	-	-	1.25	2.5" round	n
-1.09	7538	-2338	45-90	4.91	-	-	1.25	2.5" round	n
-1.06	6718	-2116	45-90	5.67	-	-	0.95	2" round pair	n
-0.86	7565	-2255	45-90	5.67	-	-	0.95	2" round pair	n
-0.89	7964	-2729	45-90	5.67	-	-	0.95	2" round pair	n
-2.02	10978	595	45-90	8.55	-	-	1.62	3" round	n
-2.09	12692	-1863	45-90	8.55	-	-	1.62	3" round	n
-0.92	13666	2017	45-90	8.55	-	-	1.62	3" round	n
-1.68	10530	-4403	45-90	8.55	-	-	1.65	3" round	n
-1.24	12031	-4070	45-90	8.55	-	-	1.65	3" round	n
-1.35	13007	-3886	45-90	8.55	-	-	1.65	3" round	n
-1.40	9342	-4018	45-90	9.82	-	-	1.25	2.5" round pair	n
-1.23	10368	-3300	45-90	9.82	-	-	1.25	2.5" round pair	n
-1.45	10660	-3598	45-90	9.82	-	-	1.25	2.5" round pair	n